

MOBI: MICROGRAVITY OBSERVATIONS OF BUBBLE INTERACTIONS

Donald L. Koch
Cornell University

Ashok Sangani
Syracuse University

One of the greatest uncertainties affecting the design of multiphase flow technologies for space exploration is the spatial distribution of phases that will arise in microgravity or reduced gravity. On Earth, buoyancy-driven motion predominates whereas the shearing of the bubble suspension controls its behavior in microgravity. We are conducting a series of ground-based experiments and a flight experiment spanning the full range of ratios of buoyancy to shear. These include: (1) bubbles rising in a quiescent liquid in a vertical channel; (2) weak shear flow induced by slightly inclining the channel; (3) moderate shear flow in a terrestrial vertical pipe flow; and (4) shearing of a bubble suspension in a cylindrical Couette cell in microgravity. We consider nearly monodisperse suspensions of 1 to 1.8 mm diameter bubbles in aqueous electrolyte solutions. The liquid velocity disturbance produced by bubbles in this size range can often be described using an inviscid analysis. Electrolytic solutions lead to hydrophilic repulsion forces that stabilize the bubble suspension without causing Marangoni stresses. We will discuss the mechanisms that control the flow behavior and phase distribution in the ground-based experiments and speculate on the factors that may influence the suspension flow and bubble volume fraction distribution in the flight experiment.

MOBI: Microgravity Observations of Bubble Interactions

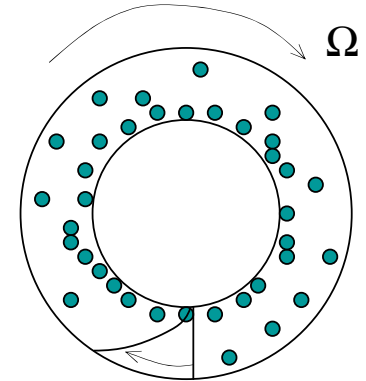
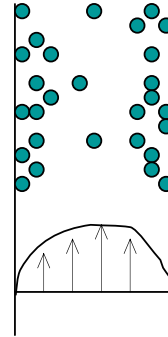
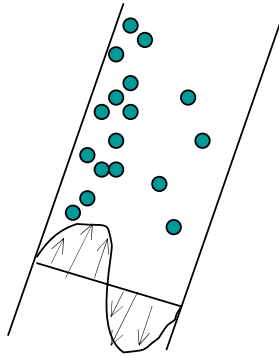
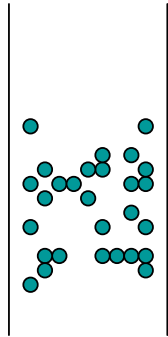
Some Thoughts on the Differences between Bubbly Flow at 1g and 0g

Donald Koch
Cornell University

Ashok Sangani
Syracuse University



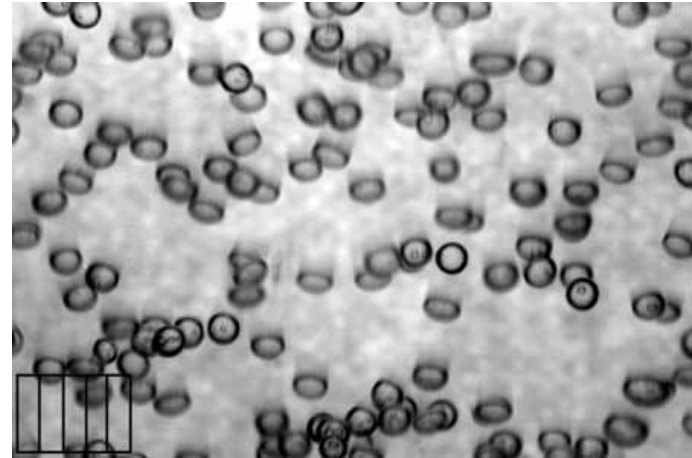
- vertical channel inclined channel vertical pipe flow Couette in μg



Increasing Ratio of Shear to Buoyancy

Monodisperse (Potential-Flow) Bubble Suspension $d \approx 1.4$ mm

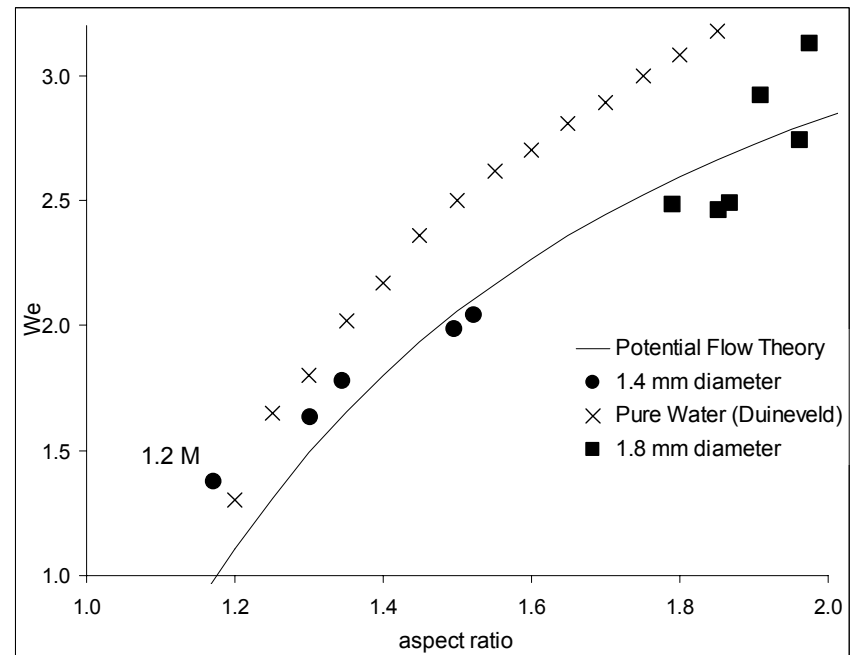
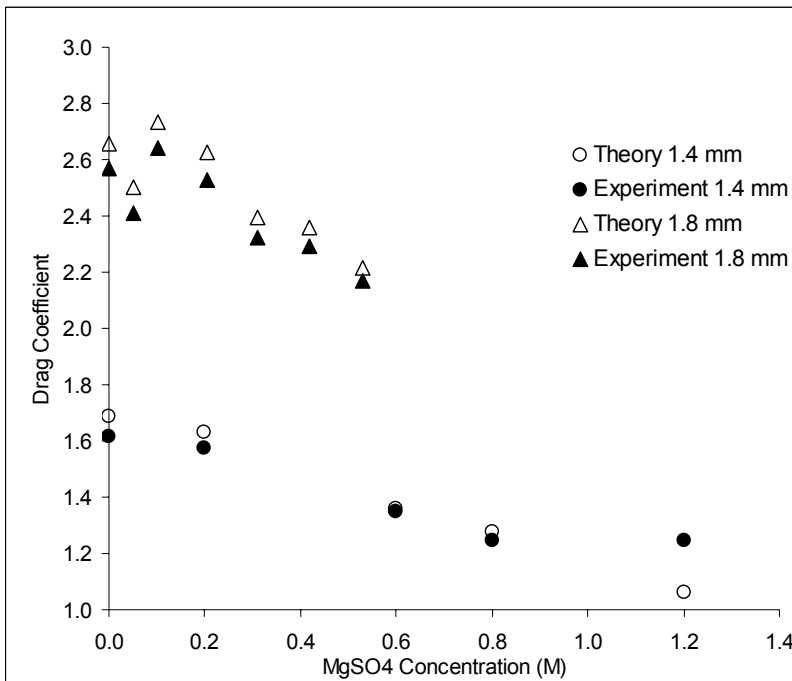
Electrolytes induce hydrophobic bubble-bubble repulsion to prevent coalescence without Marangoni stresses



Dual impedance probe: Bubble velocity and volume fraction profiles
Hot film probe: Liquid velocity
Video: Bubble size and aspect ratio

0.8 M MgSO₄ Increases Viscosity by About 60%

However, Potential Flow Theory Still Provides Accurate Predictions of Drag Coefficient and Aspect Ratio



Averaged equations for bubble suspension

- Bubble phase :

$$\frac{\partial \phi}{\partial t} + \frac{\partial}{\partial x_j} (\phi w_j) = 0$$

$$n \frac{dI_i}{dt} = - \frac{\partial P_{ij}}{\partial x_j} + n F_i^b$$

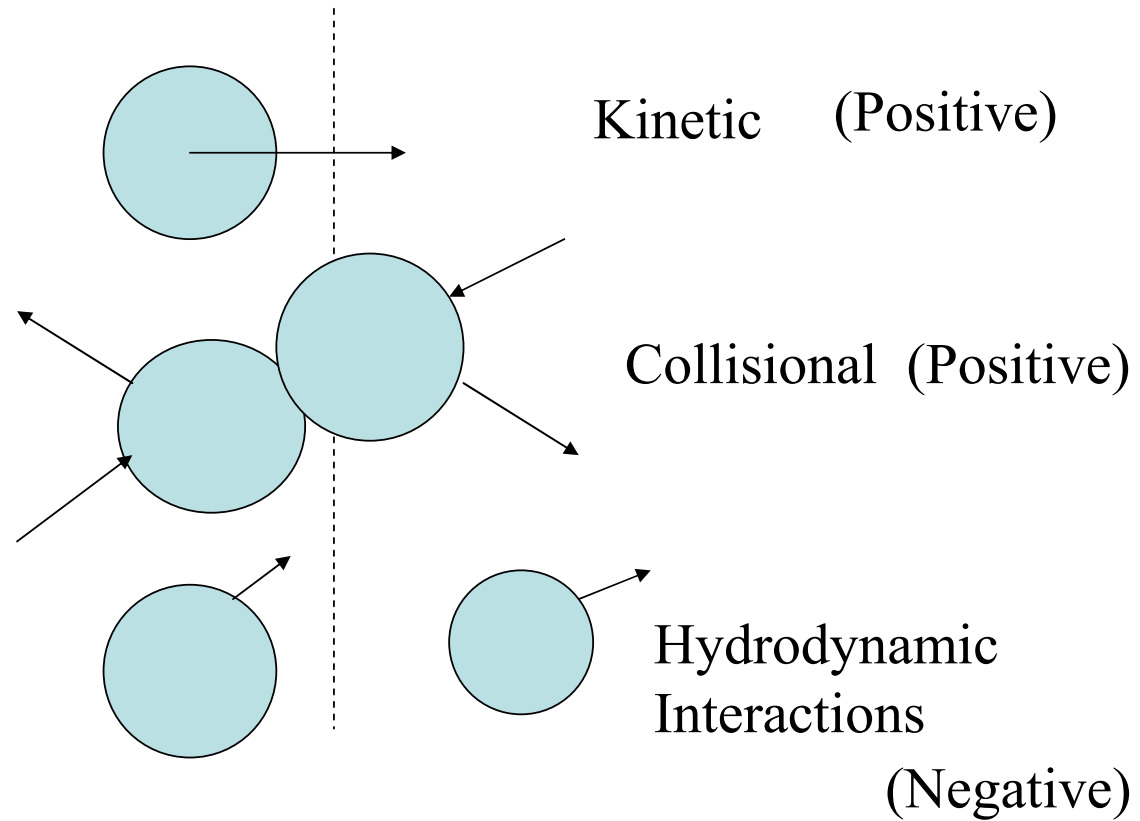
$$n \frac{dT}{dt} = - \frac{\partial Q_j}{\partial x_j} + S$$

- Entire mixture :

$$\frac{\partial u_j}{\partial x_j} = 0$$

$$\frac{\partial}{\partial t} (1 - \phi) u_i^L + \frac{\partial}{\partial x_j} (1 - \phi) u_i^L u_j^l = - \frac{1}{\rho} \frac{\partial \Sigma_{ij}}{\partial x_j} + (1 - \phi) g_i$$

Disperse-phase pressure

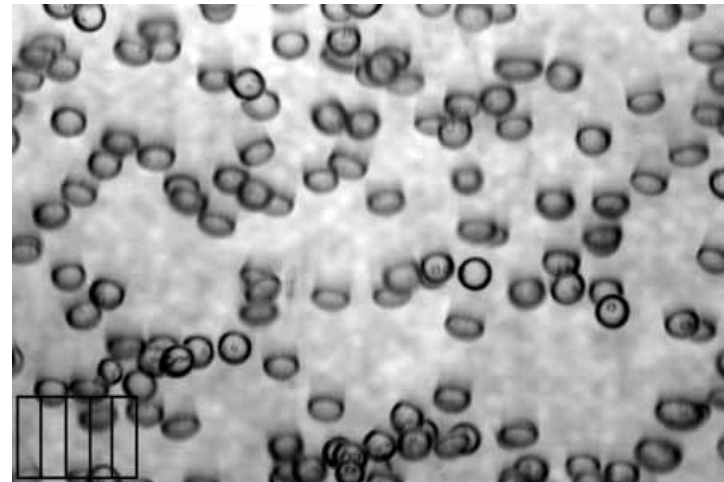
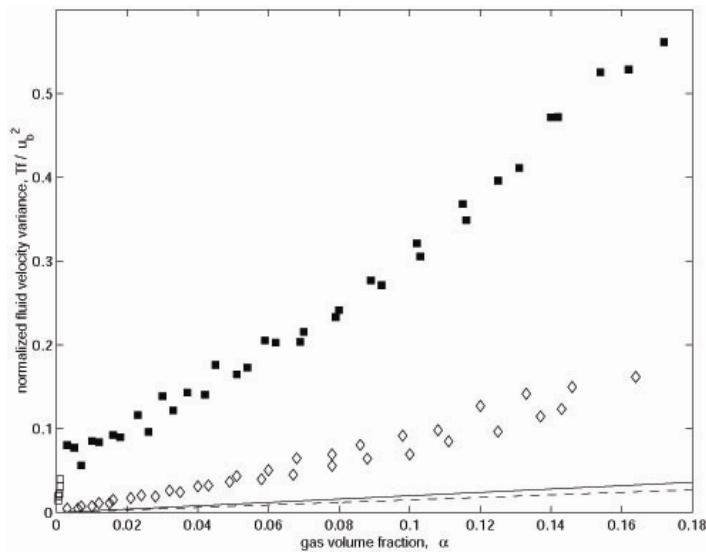


Negative pressure due to hydrodynamic interactions leads to instabilities on Earth that are absent in microgravity

Detection of Instabilities: Vertical Channel Studies

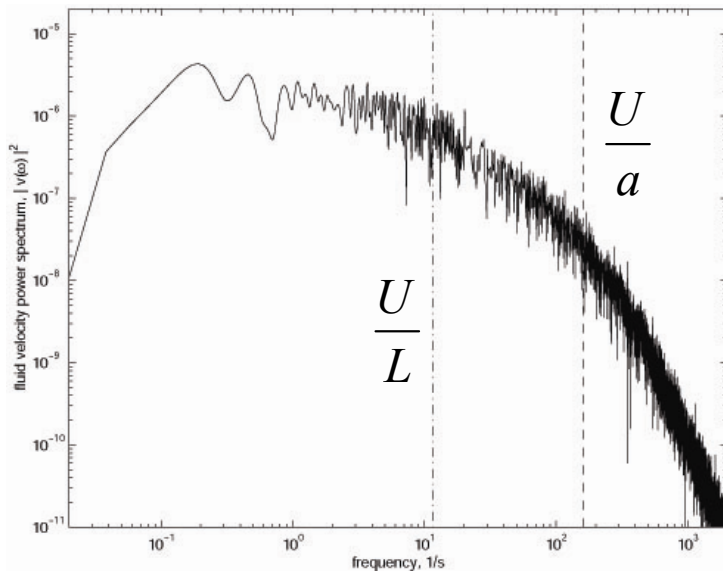
Liquid Velocity Variance
Much Larger than Expected
For Homogeneously
Distributed Potential-Flow Bubbles

Visual Evidence of Structure:
Some Horizontal Clustering

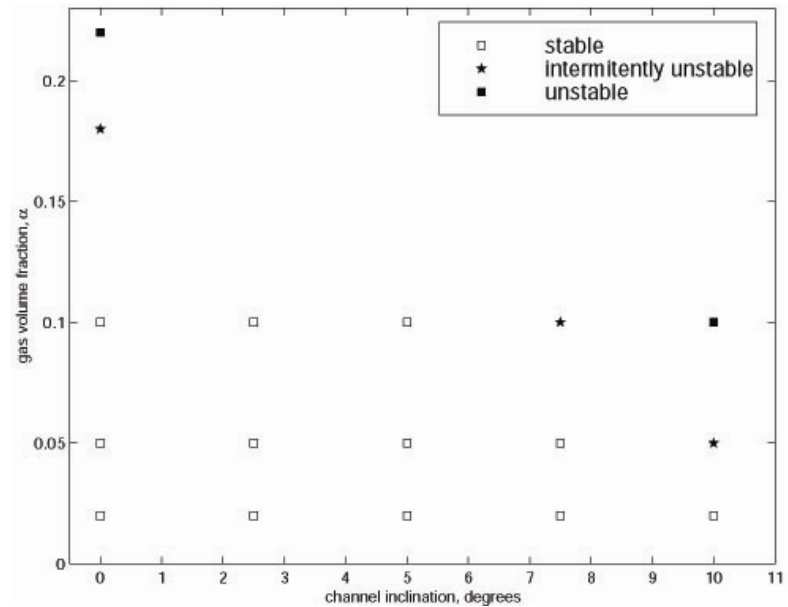


Instability in Vertical and Inclined Channel

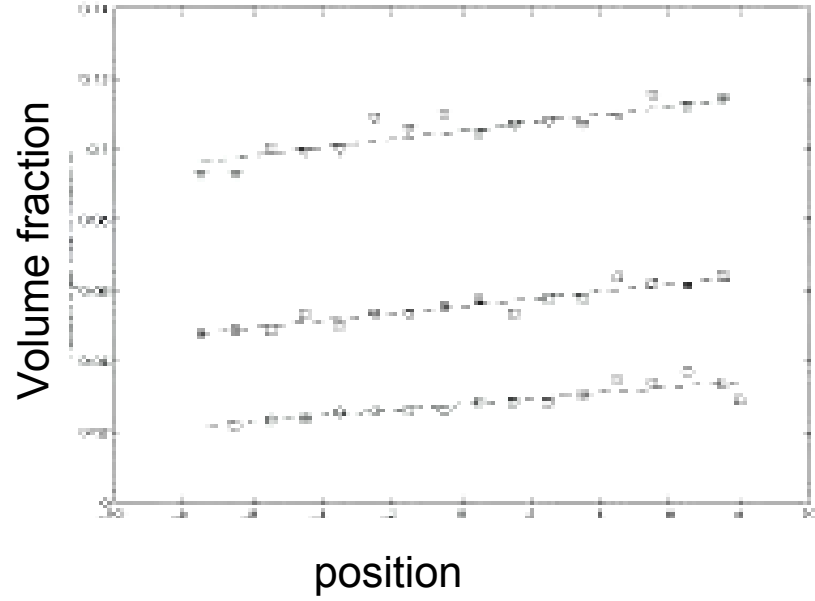
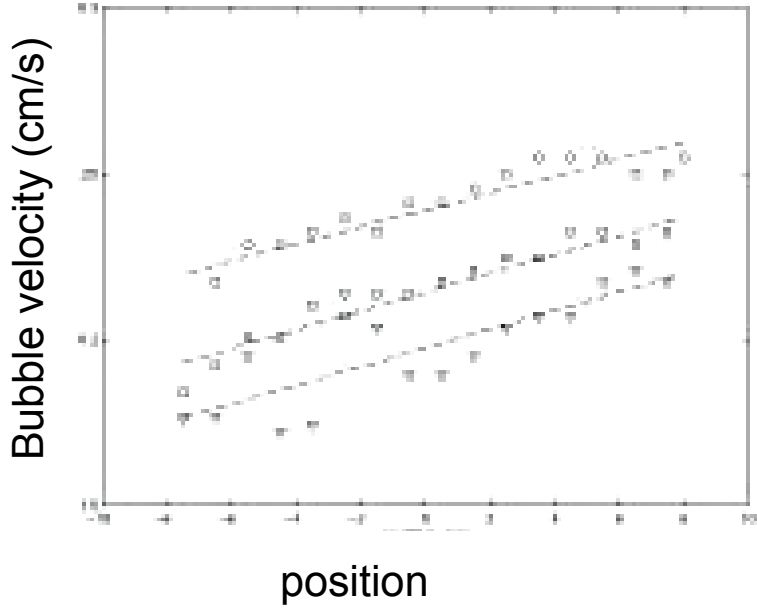
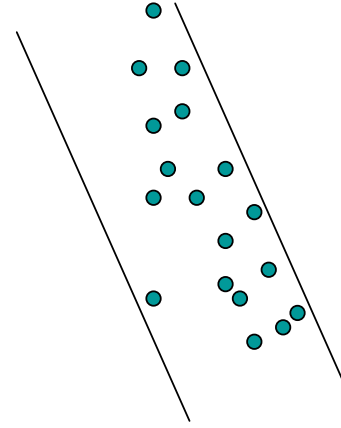
Frequency Spectrum of Liquid Velocity Shows Most of the Energy is at Frequencies Larger than U/a



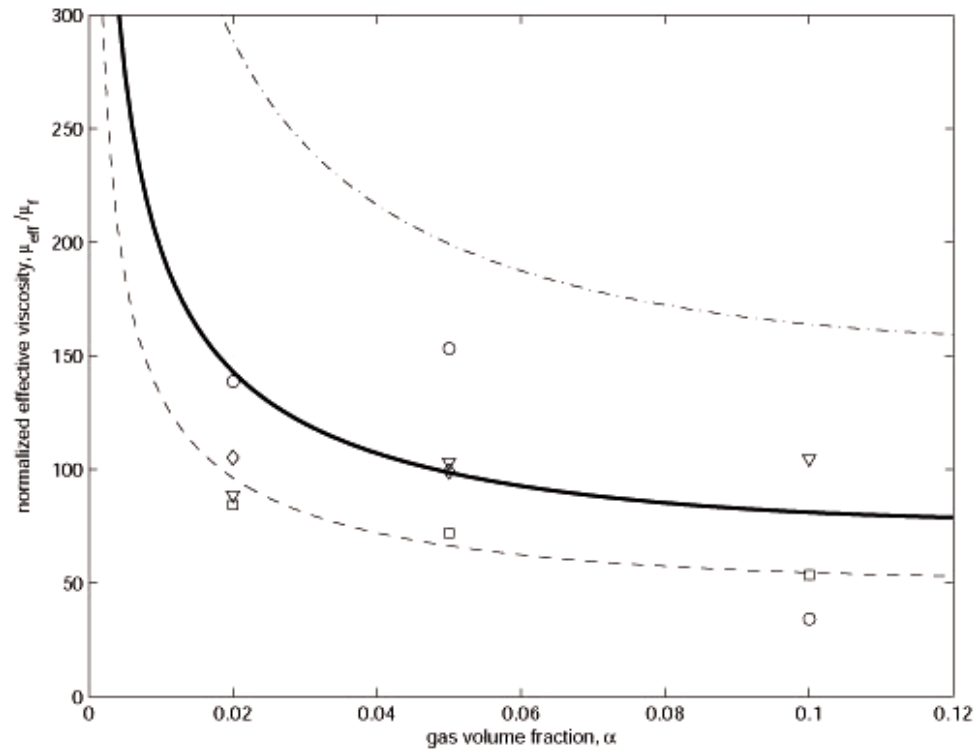
An Instability That is More Apparent to the Naked Eye Arises at Higher Volume Fractions and Inclination Angles



Inclined Channel: Bubble volume fraction variation drives suspension flow



Viscosity associated with the instability-induced Reynolds stress
 Is 100 times larger than fluid viscosity and 30 times larger than
 viscosity predicted for a homogeneous suspension

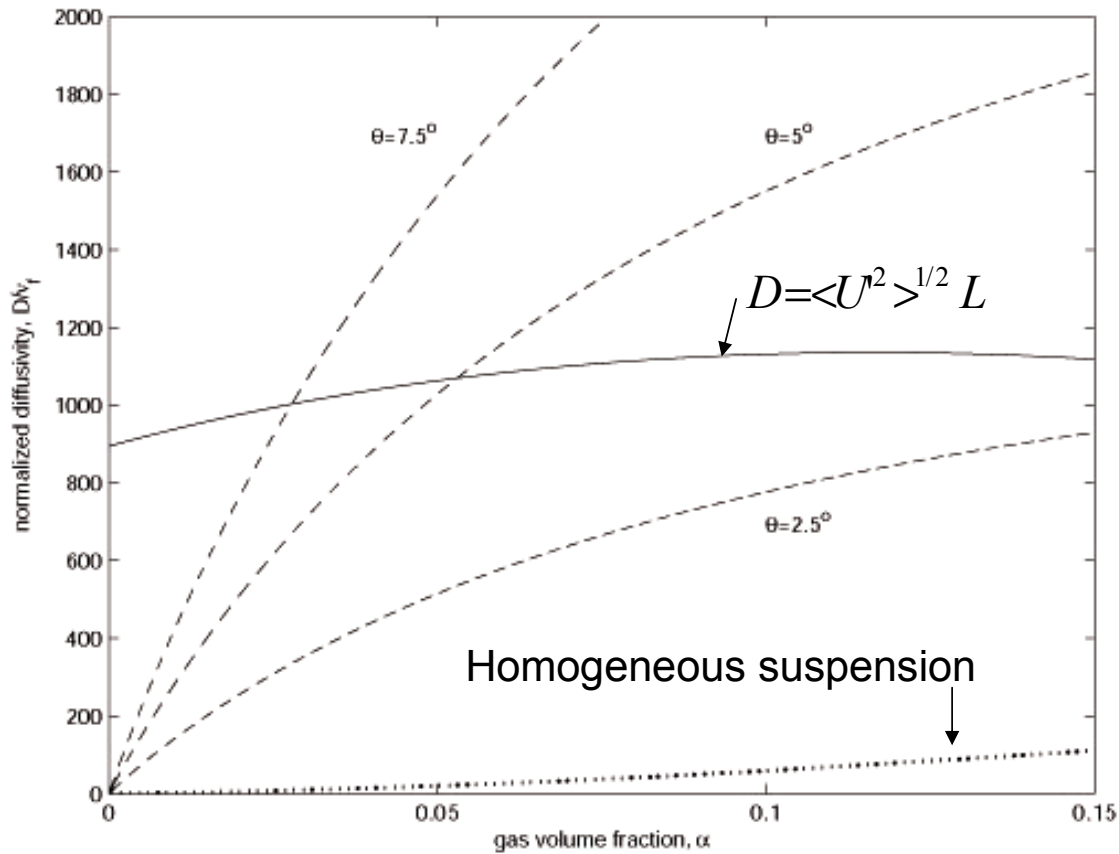


$$\nabla \cdot [\mu_{eff} \nabla \mathbf{U}] = -\rho \mathbf{g} \phi + \nabla p_f$$

Instability induced bubble pressure or diffusivity is also very large

$$n(\mathbf{F}_B + \mathbf{F}_L + \mathbf{F}_D) = \nabla P \rightarrow \nabla \cdot [(\mathbf{U}_B + \mathbf{U}_L)\phi] - \nabla \cdot [D\nabla\phi] = 0$$

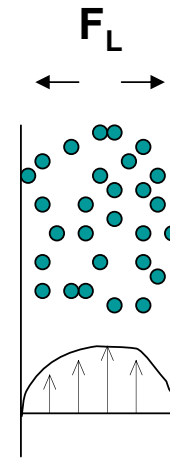
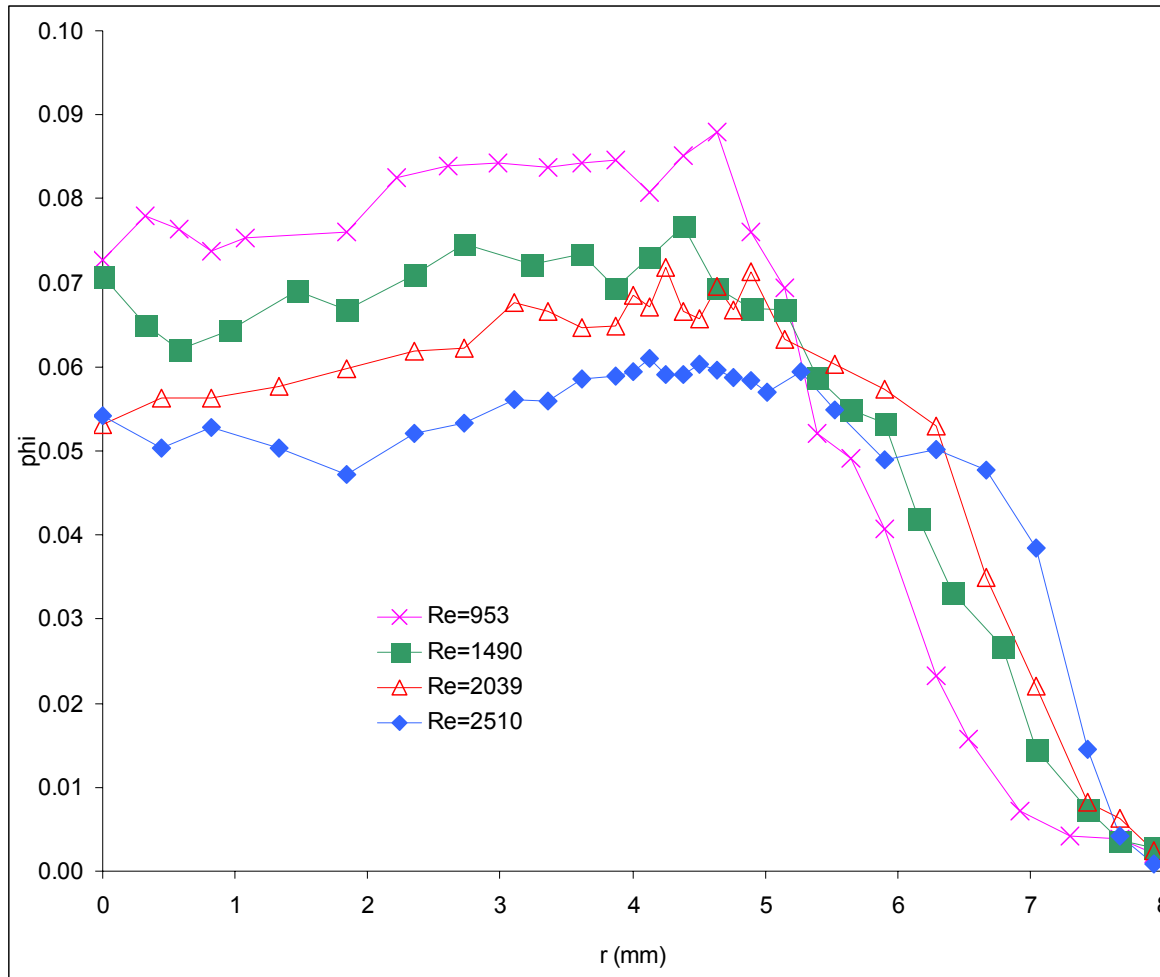
$$D = \frac{1}{36\mu_f dR_d} \frac{\partial P}{\partial \phi}$$



Apparent bubble viscosity and pressure observed in ground-based experiments in an inclined channel are greatly enhanced by an instability.

The instability results from the negative pressure due to hydrodynamic interactions which would be absent at 0g

Volume fraction profile in a vertical pipe flow



Deficit of bubbles
near pipe wall
due to repeated bubble
bouncing from wall
which would be absent
At 0g

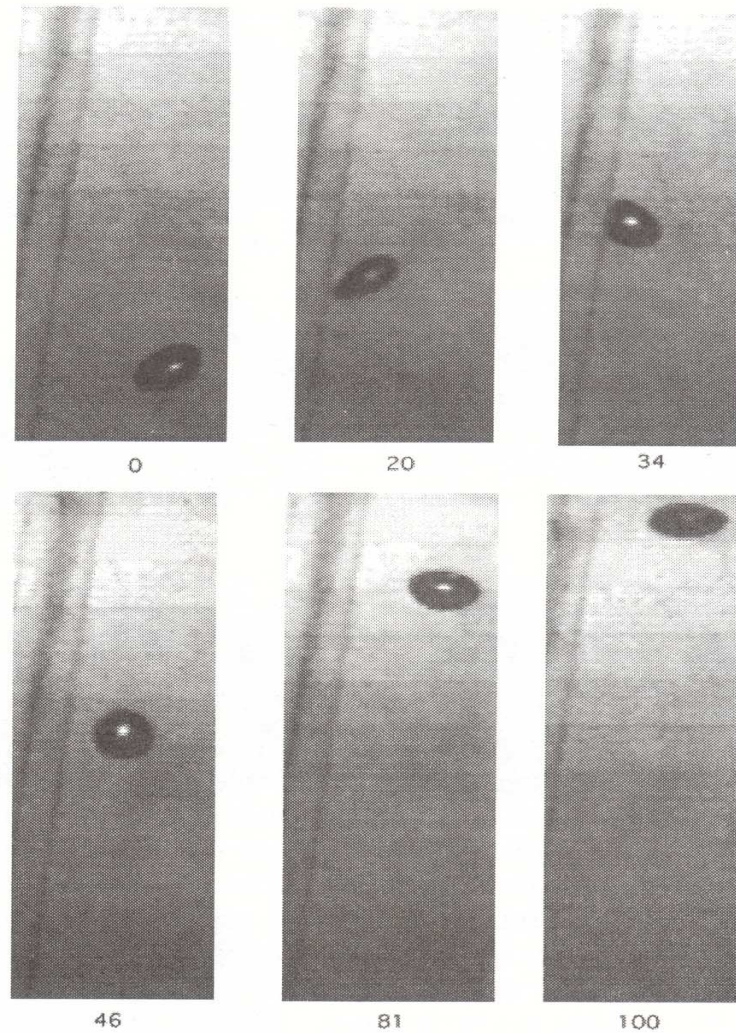


FIG. 12. Sequence of photographs illustrating one cycle of the bubble bouncing motion. The bubble radius is 0.7 mm and the inclination angle is 83°.

Couette Flow of Bubble Suspension at 0g

$$U \approx u_L$$

Gravity-induced instability absent

Repeated bouncing from wall absent

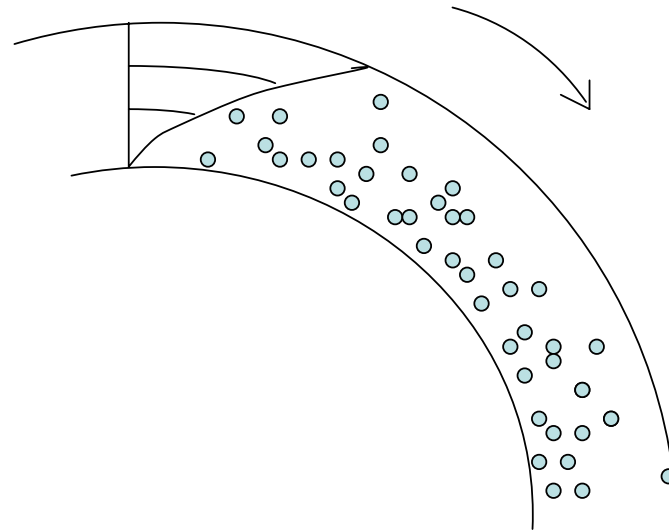
Potential flow approximation

more accurate in high Re

microgravity shear flow

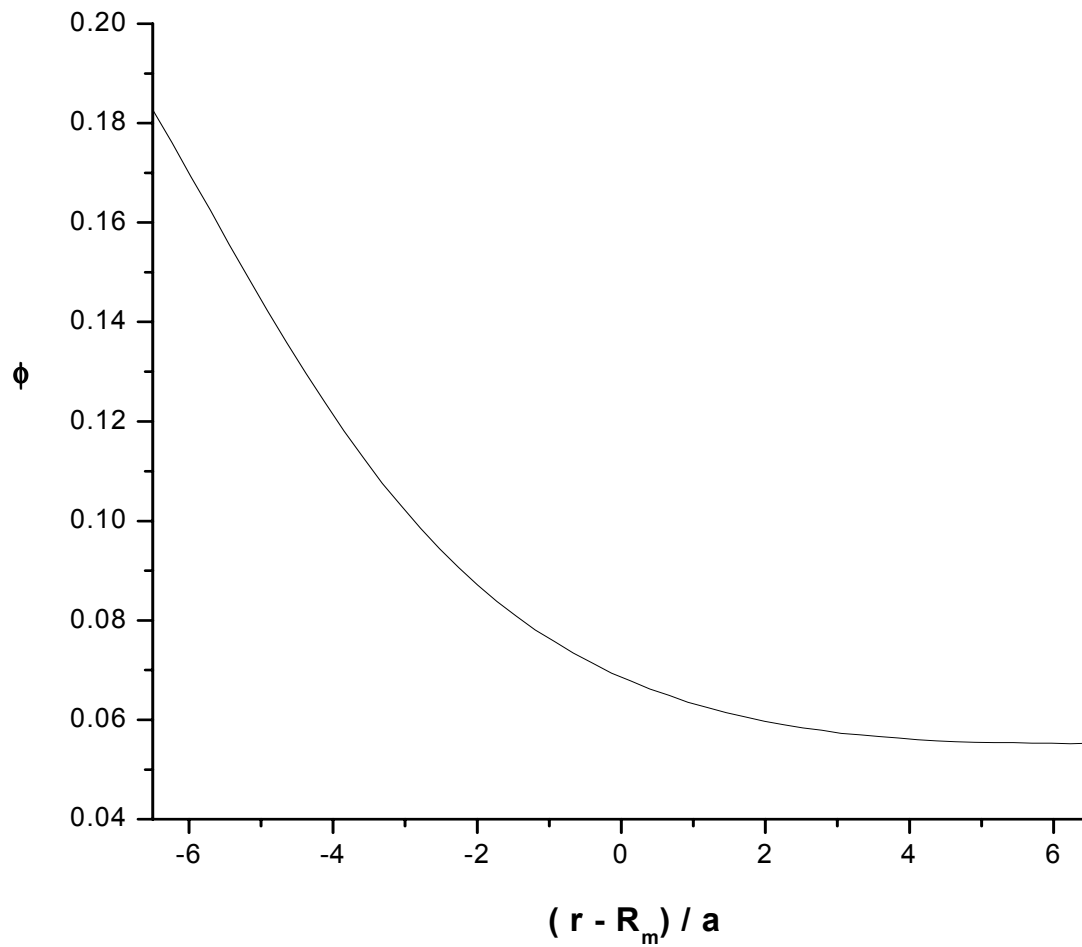
than on Earth

$$\text{Re} = \frac{\rho \Gamma a^2}{\mu_f}$$

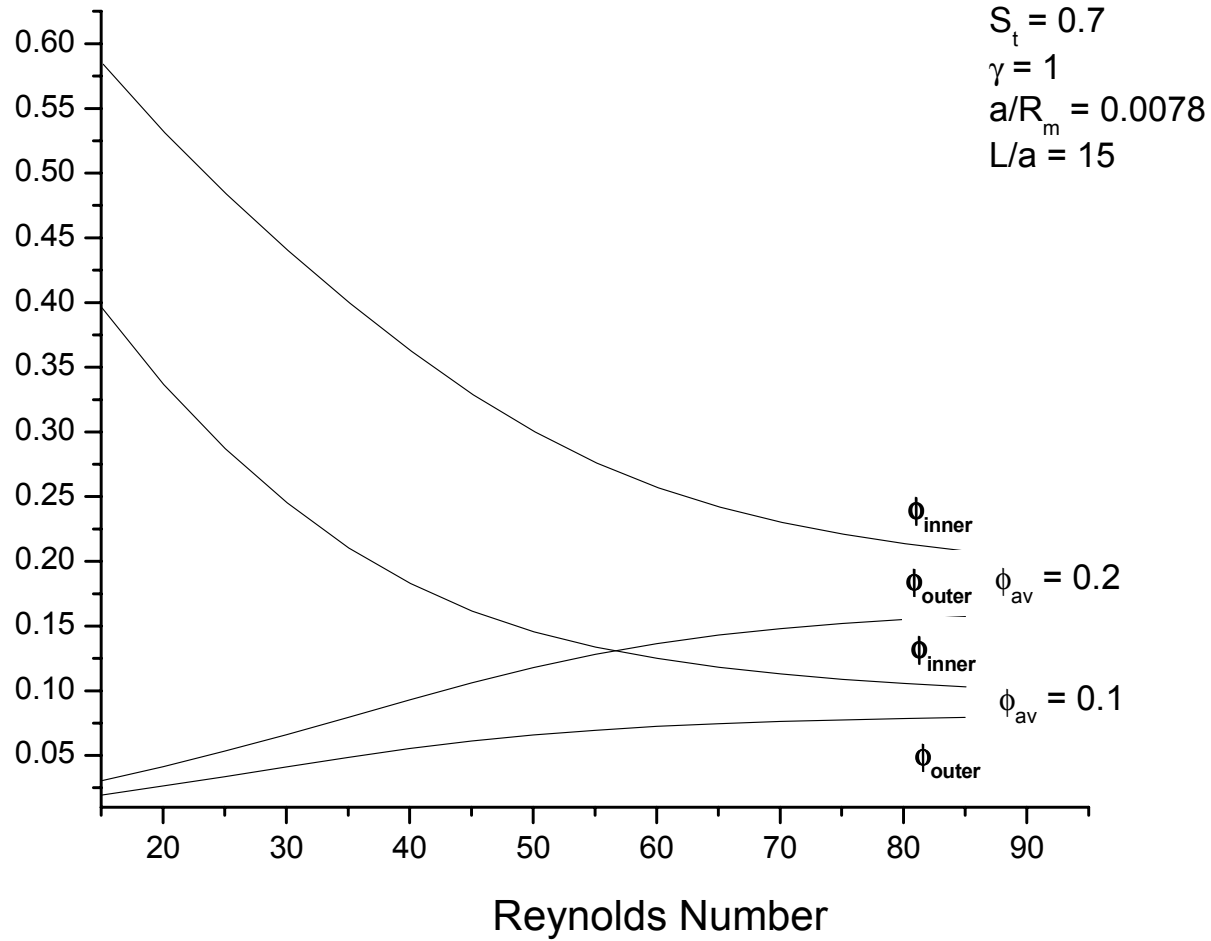


Volume fraction Profile by FEM

$S_t = 0.7$
 $\gamma = 1$
 $a/R_m = 0.0078$
 $Re = 40$

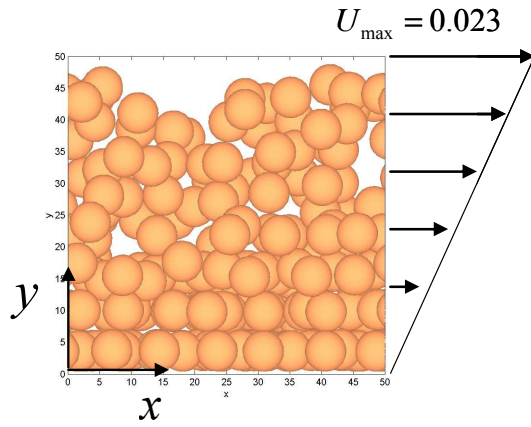


Minimum and maximum volume fractions



Lattice-Boltzmann simulations for bubble suspension
at finite Re

Bubbles modeled as non-deformable spheres
with no tangential stress boundary conditions
(specular reflection of lattice gas)

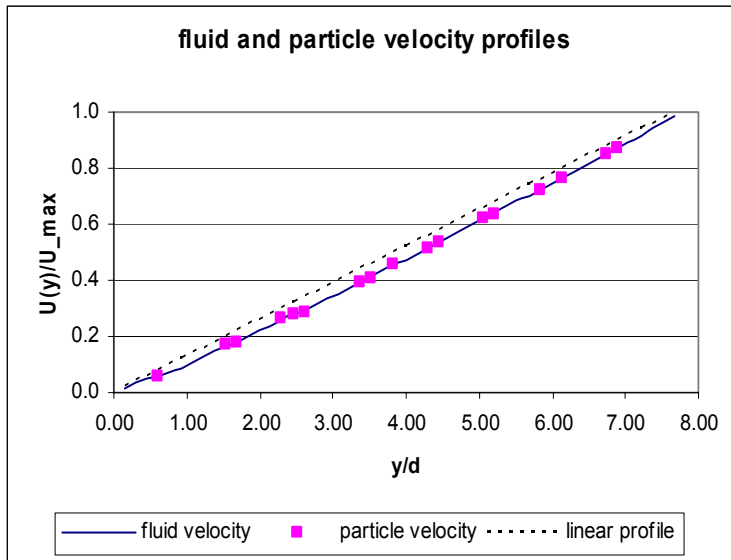
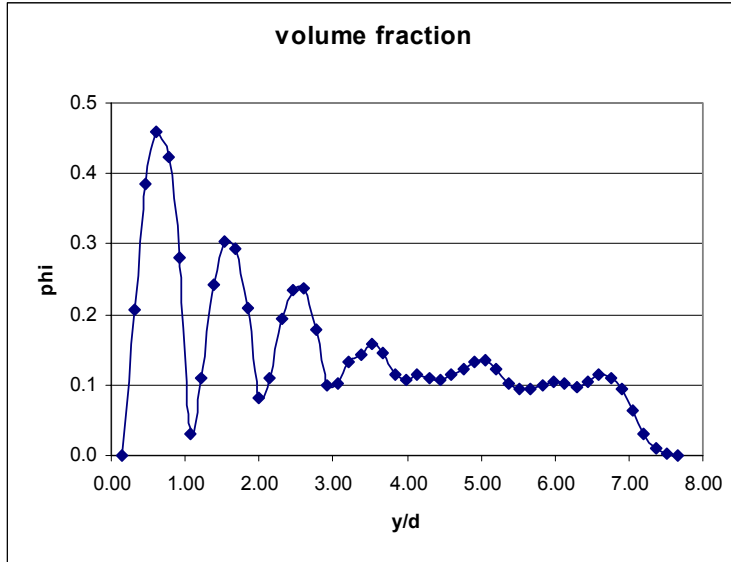


Simulation Parameters:

$R/L = 5$

$L / d = 7.67$

$Re = 0.117$



Conclusions

A buoyancy-driven instability (not readily apparent to the naked eye) greatly enhances the apparent bubble-phase viscosity and pressure in an inclined channel flow

Buoyancy driven bubble-wall interactions create a deficit of bubbles near the wall in vertical pipe flow

These effects should be absent in 0g

We predict that the bubble volume fraction distribution in microgravity Couette flow will result from a competition between bubble-phase pressure and centrifugal forces

Acknowledgements

Ying Tsang
Xiaolong Yin
Roberto Zenit

NASA grant NAG3-1853

Humpback whale courtesy of
Alaska Dept of Fish and Wildlife

